

Enhancing Urban Intersection Efficiency: Leveraging Visible Light Communication for Traffic Optimization

Manuel Augusto Vieira
*Electronics Telecommunications
 and Computer Dept.*
 ISEL, CTS-UNINOVA and LASI
 Lisbon, Portugal
 email: mv@isel.ipl.pt

Paula Louro
*Electronics Telecommunications
 and Computer Dept.*
 ISEL, CTS-UNINOVA and LASI
 Lisbon, Portugal
 email: paula.louro@isel.pt

Manuela Vieira
*Electronics Telecommunications
 and Computer Dept.*
 ISEL, CTS-UNINOVA, LASI and
 NOVA School of Science and
 Technology
 Lisbon, Portugal
 email: mv@isel.ipl.pt

Gonçalo Galvão
*Electronics Telecommunications
 and Computer Dept.*
 ISEL,
 Lisbon, Portugal
 email: A45903@alunos.isel.pt

Mário Véstias
*Electronics Telecommunications
 and Computer Dept.*
 INESC INOV-Lab,
 Lisboa, Portugal
 email: mario.vestias@isel.pt

Abstract— This paper presents a method using Visible Light Communication (VLC) to improve traffic signal efficiency and manage vehicle trajectories at urban intersections. It combines VLC localization services with learning-based traffic signal control for a multi-intersection traffic system. VLC enables communication between vehicles and infrastructure, aiding in joint transmission and data collection. The system aims to reduce waiting times for pedestrians and vehicles while enhancing safety. It's flexible, adapting to various traffic movements during signal phases. Cooperative mechanisms balance traffic flow between intersections, improving road network performance. Evaluated using the SUMO urban mobility simulator, it shows reduced waiting and travel times. An agent based scheme optimizes traffic signal scheduling based on VLC behaviors. The proposed approach is decentralized and scalable, suitable for real-world traffic scenarios.

Keywords— *Intelligent Transport System (ITS); Visible Light Communication; traffic signal control; urban intersections; traffic flow optimization; pedestrian safety; SUMO simulator; cooperative communication.*

I. INTRODUCTION

The transportation landscape is rapidly evolving with the integration of smart sensors, Visible Light Communication (VLC), and artificial intelligence. VLC, using light intensity modulation from LEDs for data transmission, shows promise in revolutionizing Smart Mobility solutions and addressing societal goals such as reducing emissions and enhancing traffic safety [1]. It is widely implemented in various domains, including vehicular communication and traffic signal systems, highlighting its versatility and efficiency. However, current traffic signal optimization often overlooks pedestrian dynamics within intersections, necessitating comprehensive systems that consider both vehicular and pedestrian flows.

This paper proposes integrating VLC localization services with learning-based traffic signal control to manage pedestrian and vehicular traffic holistically [2]. Leveraging Reinforcement Learning (RL) concepts, the system optimizes traffic flow and enhances safety by considering interactions between vehicles and pedestrians. It introduces a pedestrian mobility model tailored for outdoor scenarios, analyzing

multiple pedestrian behaviors, and incorporating them into the traffic signal control scheme. Validated through a case study in Lisbon's downtown, the model integrates pedestrian preferences to optimize routing algorithms [3].

Simulation experiments validate the effectiveness of the approach, utilizing real intersection data to demonstrate improved traffic flow and reduced waiting times.

The paper is structured to discuss, in Section 1, the importance of traffic control, in Section 2, the challenges it faces, and the motivation behind the proposed solution. It then delves, in Section 3, into the complexities of managing traffic in multi-intersection environments and, in Section 4, presents a model for traffic signal control incorporating machine learning elements, and analyzes simulated results. Finally, the conclusions, in Section 5, summarize the findings, insights gained, limitations, and potential future directions of the research.

II. TRAFFIC CONTROL CHALLENGES

A. Pedestrian Dynamics and Complexity in Multi-Intersection Environments

Traffic signal control research has traditionally prioritized vehicles, but there's now a shift towards pedestrian-friendly systems to prevent delays and accidents [4][5]. Sidewalks present challenges due to bi-directional flow, and differing speeds and movements between pedestrians and vehicles further complicate matters [6]. Our adaptive traffic control considers factors like queue lengths in neighboring intersections to balance scalability and efficiency. Our strategy is designed to address real-time traffic demands by modeling current and anticipated future traffic flows. Compared to traditional fixed coil detectors, our adaptive system in V2X environments gathers more granular data, including vehicle positions, speeds, queue lengths, and stopping times. V2V links play a crucial role in safety functionalities like pre-crash sensing, while V/P2I links provide valuable information to connected vehicles.

B. Integrating V-VLC for Innovative Traffic Solutions

With wireless tech advancements and Connected Vehicle (CV) [7] systems like V2V and V2I, integrating VLC localization with learning-based traffic control can manage both pedestrian and vehicular traffic in multi-intersections. It employs RL to enhance safety and reduce waiting times using V2V, V/P2I, and I2V/P communications. This approach synchronizes signal control in real-time, considering pedestrian and vehicle factors in the state and reward design, utilizing sidewalks for crucial pedestrian location info. SUMO simulations [8] assess the V-VLC system's effectiveness, with agent-based models learning to optimize traffic flow dynamically. Dynamic diagrams and state matrices illustrate the concept, showing potential for optimal traffic control policies.

III. UNLOCKING TRAFFIC CONTROL

A. VLC background

The V-VLC system, as depicted in Figure 1a, utilizes a mesh cellular hybrid structure with two controllers. The "mesh" controller at streetlights relays messages to vehicles, while the "mesh/cellular" hybrid controller acts as a border-router for edge computing [9][10].

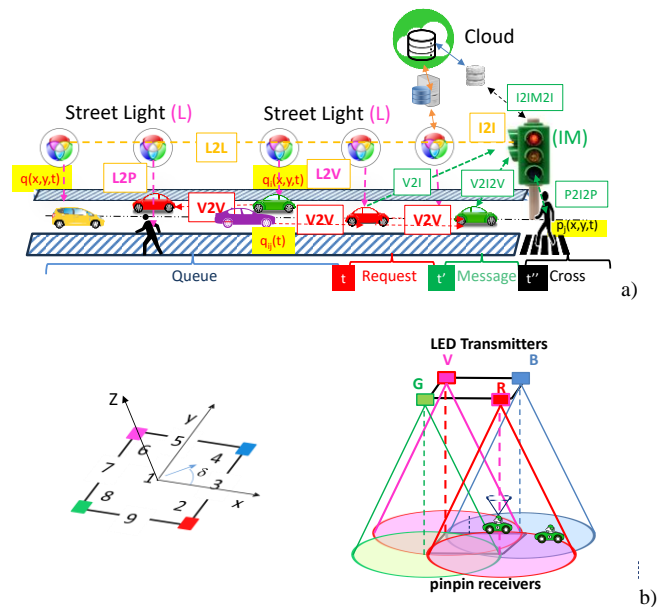


Figure 1. a) 2D representation of the simultaneous geo-localization as a function of node density, mobility and transmission range. b) Emitter and receivers' relative positions. Illustration of the coverage map in the unit cell: footprint regions (#1-#9) and steering angle codes (2-9).

The proposed architecture enables Infrastructure-to-Cloud communication (I2IM) through embedded computing platforms for processing and sensor interfacing. It also facilitates peer-to-peer communication (V2V) among vehicles, enhancing data sharing.

The Vehicular Visible Light Communication system (V-VLC) consists of a transmitter generating modulated light and a receiver detecting light variation, both wirelessly connected. LED-produced light is modulated using ON-OFF-keying (OOK) amplitude modulation (Figure 1b). Square unit cells in the environment feature tetra-chromatic white light (WLEDs) sources at cell corners. The V-VLC system uses coded signals transmitted by devices like streetlights, headlights, and traffic

lights to communicate directly with identified vehicles and pedestrians (L/I2V/P), or indirectly between vehicles through their headlights (V2V). PIN-PIN photodetectors within mobile receivers receive and decode coded signals. This information aids in pinpointing positions within the network and provides directional guidance along cardinal points for drivers/pedestrians [10].

The system employs queue/request/response mechanisms and temporal/space relative pose concepts to manage vehicle passage through intersections. Vehicle speed is determined using transmitter IDs for tracking, while mesh nodes estimate indirect V2V relative poses in scenarios with multiple neighboring vehicles.

The integration of VLC enables direct monitoring among pedestrians, vehicles, and infrastructure, focusing on critical aspects such as queue formation and pedestrian corner density to enhance road safety. P2I2P communication enables travel time calculations, while real-time data on speed and waiting times are analyzed using transmitter tracking IDs.

B. Traffic Scenario and Phasing Diagram

The simulated scenario, as shown in Figure 2a, features two intersections, each with two 4-way junctions, consisting of 2 lanes per arm spanning 100 meters in total length.

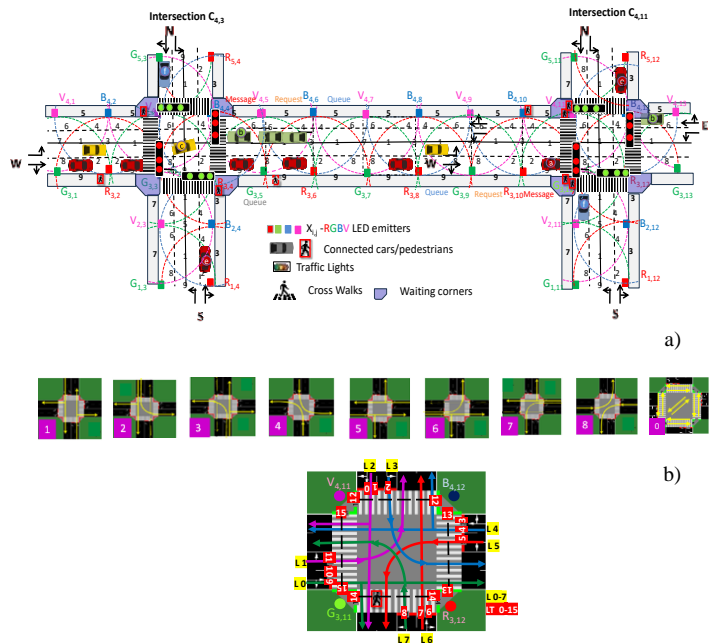


Figure 2. Simulated scenario: Four-legged intersection and environment with the optical infrastructure (X_{ij}), the generated footprints (1-9) and the connected cars and pedestrians. b) Phasing diagram and schematic diagram of the C2 intersection with coded lanes (L/0-7) and traffic lights (TL/0-15).

Traffic flows from compass directions, with lanes indicating movement options: right lanes for right turns or going straight, and left lanes for left turns only. Central traffic light systems, regulated by Intelligent Managers (IMs), control traffic. Features like emitters (streetlamps), pedestrian lanes, waiting areas, and crosswalks are integrated. Four traffic flows along cardinal points are considered, with road request and response segments offering binary choices (turn left/straight or turn right). Assumptions include a total influx of 2300 cars per hour, primarily from east and west directions, with 25% expected to turn and 75% to continue straight. Pedestrian influx is around 11200 per hour, crossing in all directions at an average speed of 3 km/h. Figure 2b outlines intersection phase progressions within a structured cycle

length, comprising eight vehicular phases and an exclusive pedestrian phase. Each phase is subdivided into discrete time sequences, providing a comprehensive temporal framework [11][12].

Each flow (illustrated by the different vehicle colors) comprises vehicles moving straight or making left turns, with specific vehicles representing top requests in the sequence. The assumption is that specific vehicles, labeled $a_1, b_1, a_2, b_2, a_3, c_1, b_3, e_1, a_4, c_2, a_5,$ and f_1 , represent the top requests in the given sequence.

C. Communication protocol, coding, and decoding techniques

Data transmission in the VLC system follows a synchronous approach using a 64-bit data frame structure. Information is encoded using On-Off Keying (OOK) modulation, with each luminaire containing WLEDs (RGBV), enabling simultaneous transmission of four signals. A PIN-PIN demultiplexer decodes the message based on calibrated amplitudes of RGBV signals. The communication protocol includes components like Start of Frame (SoF) for synchronization, Identification Blocks encoding communication type (COM) and localization (position, time), and other ID Blocks for additional identifiers, Traffic Message containing vehicle information, and End of Frame (EoF) indicating the end of transmission. This structured protocol ensures efficient encoding and decoding of critical movement information, maintaining synchronization and data integrity in the VLC system. In Table 1, the communication protocol is depicted.

TABLE I. COMMUNICATION PROTOCOL.

	COM	Position		ID (veic)	Time			payload			EOF	
		x	y		END	Hour	Min	Sec	Car IDx	Car IDy		nr behind
I2V	Sync	1	x y	0 bits	END	Hour	Min	Sec				EOF
V2V	Sync	2	x y	Lane (0-7) Veic. (nr)	END	Hour	Min	Sec	Car IDx	Car IDy	nr behind	EOF
V2I	Sync	3	x y	TL (0-15) Veic. (nr)	END	Hour	Min	Sec	Car IDx	Car IDy	nr behind	EOF
I2V	Sync	4	x y	TL (0-15) ID Veic.	END	Hour	Min	Sec	Car IDx	Car IDy	nr behind	EOF
P2I	Sync	5	x y	TL (0-15) Direct.	END	Hour	Min	Sec				EOF
I2P	Sync	6	x y	TL (0-15) Phase	END	Hour	Min	Sec				EOF

Decoding the information received from the photocurrent signal captured by the photodetector involves a critical step reliant on a pre-established calibration curve [12]. This curve meticulously maps each conceivable decoding level to a sequence of bits. Essentially, the calibration curve serves as a guide, facilitating the establishment of associations between photocurrent thresholds and specific bit sequences.

IV. RESULTS

A. VLC Algorithms

Figure 3, displays the decoded optical signals (at the top of the figures) and the signals received (MUX) by the receivers in a V2V (COM 2) and V2I (COM 3) communication scenario involving a leader vehicle a_0 at position $(R_{3,10}, G_{3,11}, B_{4,10})$. This vehicle is communicating with the agent at the second intersection (C2) on lane L0 (direction E) at 10:25:46 and is followed by three other vehicles (Veic. nr) $V_1, V_2,$ and V_3 with the same direction, located at positions $(IDx, y) R_{3,8}, G_{3,6}$ and $R_{3,4}$, respectively.

Figure 4 demonstrates the MUX signal and the decoded messages sent by the traffic lights to pedestrians (I2P_{1,2}). This

visual representation helps to understand the communication between pedestrians waiting in the corners and the corresponding traffic lights, providing insights into the signals exchanged for pedestrian crossings at both intersections (C1 and C2).

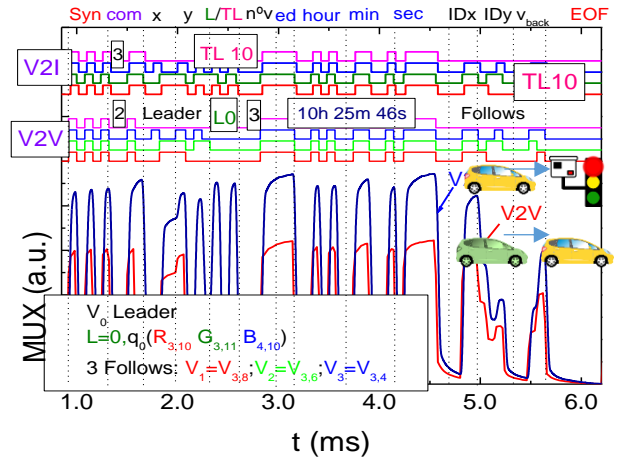


Figure 3. MUX signal request assigned to different types of communication. On the top the decoded messages are displayed.

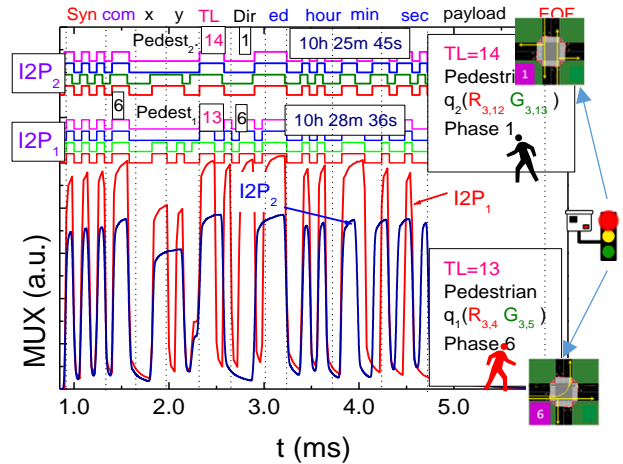


Figure 4. Normalized MUX signal responses and the corresponding decoded messages, displayed at the top, sent by the IM to pedestrians waiting in the corners (I2P_{1,2}) (b) at various frame times.

Upon pedestrian q_2 receiving information from the traffic light C2, it becomes evident that the current active phase is N-S (Phase 1), signifying that the pedestrian did not arrive in time for their designated phase (Phase 0). Consequently, the pedestrian is required to wait for an estimated cycle time of 3 (cycle time) minutes before being granted the opportunity to cross. Subsequently, the pedestrian crosses the crosswalk, covering the distance to the next intersection in approximately 1 minute and 50 seconds. Upon arrival, the pedestrian waits in the designated waiting zone at position $R_{3,4}-G_{3,5}$ until the pedestrian phase becomes active once again. At 10:28:35, the pedestrian establishes communication with traffic light TL13 at the C1 (P12I). The traffic light promptly responds (I2P₁) at 10:28:36, providing crucial information that the currently active phase is the final one in the cycle (Phase 6). These interactions highlight the effectiveness of the pedestrian's communication with the

traffic lights, enabling them to stay informed about the active phase, waiting time, and make decisions accordingly.

B. Dynamic Traffic Control: Integrating Pedestrian Consideration

Assessing the effectiveness of the proposed V-VLC system in multi-intersection utilizes the Simulation of Urban MObility (SUMO), employing agent-based simulations. SUMO tests traffic control algorithms, manages intersections, and oversees pedestrian crossings, mirroring real-world conditions. For data analysis, SUMO collects and analyzes simulation data, including vehicle trajectories, travel times, congestion levels, and pedestrian movements.

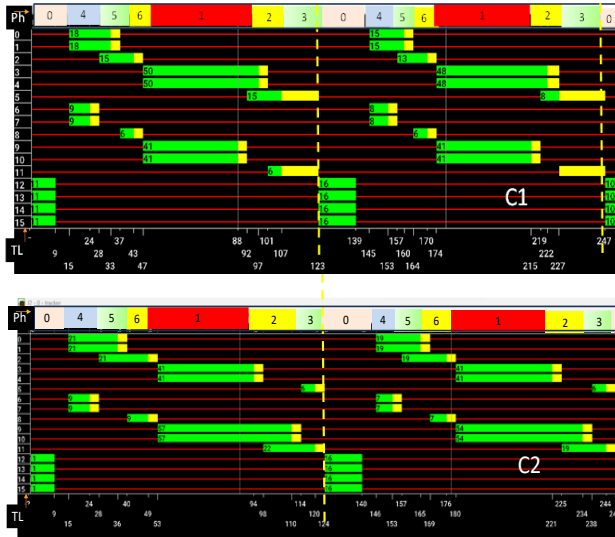


Figure 5. State phasing diagrams for C1 and C2 intersections.

The simulation scenario, adapted to the SUMO simulator, provides insights into traffic light signals and vehicle/pedestrian movements within the terminals. In Figure 5 a state diagram was generated for C2 intersection, incorporating both vehicles in the lanes (2300v/h) and pedestrians (11200 p/h) in the sidewalks during two cycles of 120 seconds. These diagrams offer insights into the dynamic behavior of traffic light signals and carrier/pedestrian movements within the simulated terminals. As can be observed in the diagrams it is possible to distinguish the different cycles that occur during the simulation. It always begins with a pedestrian phase (Phase 0), during which some pedestrians can cross the crosswalk, turning red for pedestrians starting from 11 seconds. Then, phases dedicated to vehicles (Phases 1-8) take place until it concludes at 123 seconds. At this moment, the second cycle begins, with the pedestrian phase becoming active again. The same process repeats until 247 seconds, marking the end of this second cycle and the initiation of a third cycle. These diagrams align with the analysis conducted for pedestrians.

V. INTELLIGENT TRAFFIC CONTROL SYSTEM

With the data collected on vehicles via VLC through the cells in Figure 1, implemented via lamps along the roads as shown in Figure 2, an intelligent traffic system must be developed to optimize traffic flow at intersections. This system utilizes Reinforcement Learning (RL), a machine learning paradigm where an agent learns to make decisions by interacting with its environment. Agents in RL aim to achieve a goal in uncertain, potentially complex environments by

receiving feedback in the form of rewards or punishments. The fundamental idea is for the agent to learn optimal behavior or strategies through trial and error.

At each time step t , the agent receives a state input s_t , based on the observation of the environment and then executes an action a_t , that transforms the state observed to a next state s_{t+1} . Then the reward r_t , a metric that defines how good the action was for the environment, is calculated. In this case, the reward is defined by (1), using the accumulated total waiting time, $atwt_t$, as a metric for vehicles (*veh*) and pedestrians (*ped*). $atwt_t$ and $atwt_{t-1}$ are the accumulated total waiting time of all the cars/pedestrians in the intersection captured respectively at agentstep t and agentstep $t-1$. The weights of the p_{veh} and p_{ped} are set based on the desired priority that the agent should have towards vehicles and pedestrians during network training. The agent will learn a policy that benefits one more than the other, or keeps the system balanced if the weights are equal.

If the agent's behavior leads to positive environmental reward, which indicates that the waiting time is longer in the past, $t-1$, than at the present moment, t , then the tendency of producing this behavior by the agent will be strengthened, and vice versa. The goal is to maximize the cumulative discounted reward.

$$r_t = p_{veh}(atwt_{veh,t-1} - atwt_{veh,t}) + p_{ped}(atwt_{ped,t-1} - atwt_{ped,t}) \quad (1)$$

This experience $e_x = (s_t, a_t, r_t, s_{t+1})$ will be stored in the replay memory, to be used in the future to train the agent. The replay memory is a dataset of an agent's experiences $D_t = (e_1, e_2, \dots, e_t)$, which are gathered when the agent interact with the environment as time goes by ($t = 1, 2, \dots, n$).

To train the agent, the deep Q-Learning technique is employed, leveraging the Q-Learning algorithm [11][13]. The Q-value represents the expected cumulative reward of taking a particular action in a particular state and following the optimal policy thereafter. These Q-values are predicted by a Neural Network (NN) that takes the state as input and outputs Q-values for each possible action.

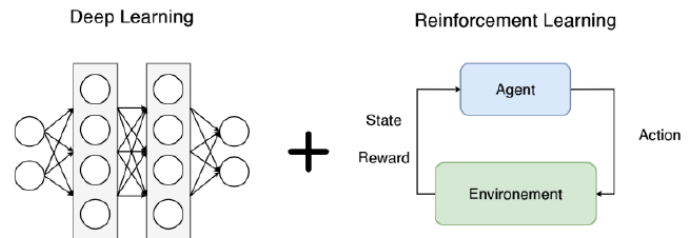


Figure 6. Deep Reinforcement Learning.

The Q-value represents the expected cumulative reward of taking a specific action in each state while following the optimal policy thereafter.

A Neural Network (NN) predicts these Q-values by taking the state as input and outputting Q-values for each possible action. The state of the environment comprises 100 cells at each intersection, indicating the presence of vehicles or pedestrians. These cells are set to '1' if occupied and '0' if not. Each lane, divided into 10 cells, indicates vehicle movement toward the intersection, with cell sizes increasing farther from the intersection. With 8 lanes per junction, there are 80 vehicle cells per intersection. For pedestrians, only the waiting zones are considered, each divided into 5 cells, totaling 20 pedestrian cells per intersection, as drafted in Figure 6.

The neural network's input layer consists of 100 neurons representing the state of the environment. This is followed by five hidden layers, each with 400 neurons using Rectified

Linear Units (ReLUs). The output layer features nine neurons, each representing the Q-values for potential actions. To refine Q-value predictions, a Mean Squared Error (MSE) function quantifies the disparity between predicted and target Q-values, enhancing the learning process. N represents the number of samples stored in memory, and Q_{target} and Q_{pred} denote the target and predicted values, respectively. After each training episode, target Q-values for action-state pairs are calculated based on (2).

$$MSE_{Loss} = \frac{1}{N} \sum_{i=1}^N (Q_{target} - Q_{pred})^2 \quad (2)$$

N is the number of samples stored in memory, and the target and predicted value, Q_{target} and Q_{pred} , respectively. After each episode of training, the target Q-values for action-state pairs are calculated based on (3).

$$Q_{target} = r_t + \gamma \cdot \max Q_{pred}(s_{t+1}, a') \quad (3)$$

The nine Q-values at the neural network's output correspond to the nine actions shown in Figure 7. The agent selects the action that best suits the current traffic situation, without following a predefined order. Conversely, today's dynamic traffic systems at junctions follow a fixed sequence of phases, as shown in Figure 7.

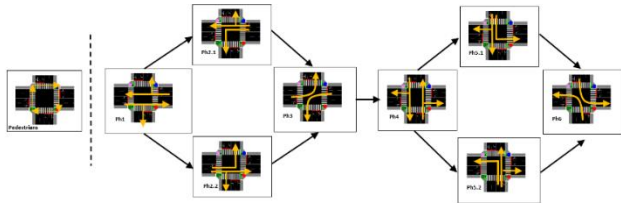


Figure 7. Nine possible actions that can be chosen by the agent.

This can result in activating a phase that does not align with current traffic needs. The next section compares these two systems to highlight their differences and evaluate their effectiveness.

VI. SIMULATION RESULTS

A. Training Results

To evaluate the behaviour of the intelligent traffic control system in relation to pedestrian and vehicle scenarios, a comparison was made with the dynamic traffic control system. The neural network used was trained with a reward system that weighted the waiting times for vehicles (p_{veh}) and pedestrians (p_{ped}) equally, for 300 epochs, each lasting one hour. Both systems considered the same generation rates for pedestrians and vehicles, totalling 2300 vehicles and 11000 pedestrians in the traffic scenario.⁸

Figure 8 shows the cumulative negative reward from training the network for both agents. Both agents evolved and learned from their traffic experiences throughout the episodes. The curves converged towards less negative reward values, indicating better decision-making over time.

In Figure 9a, which represents the high vehicle and pedestrian scenario, the intelligent system significantly outperforms the dynamic system. The dynamic system peaks at around 1500 waiting pedestrians in the first 25 minutes, while the intelligent system peaks at just 400 pedestrians. Figure 9b shows a smaller difference in the high vehicle and low pedestrian scenario, where the dynamic system peaks at 275 pedestrians in the first 15 minutes, compared to 150 for the intelligent system. This disparity arises because the

intelligent system adapts phases dynamically to current traffic conditions, unlike the dynamic system, which follows a fixed cycle. The pedestrian phase in the dynamic system, appearing every 120 seconds, results in periodic peaks in waiting pedestrians.

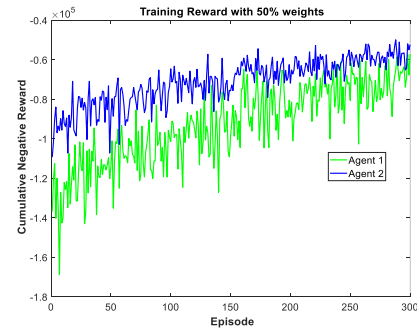


Figure 8. Cumulative Negative reward for both agents in training.

After training the network, tests were conducted to compare both systems under two traffic scenarios representing peak hour conditions. The first scenario involved high vehicle and pedestrian traffic (High-High) with 2300 cars and 11000 pedestrians. The second scenario had high vehicle traffic but low pedestrian traffic (High-Low), with 2300 cars and 5600 pedestrians.

B. Testing results – High-High and High-Low scenarios

Figures 9a and 9b display the number of pedestrians waiting in zones at the two junctions for both traffic scenarios.

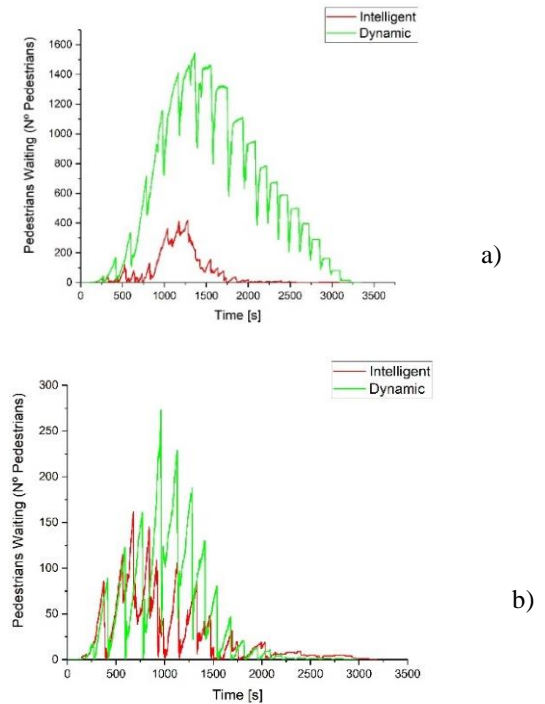


Figure 9. Comparison of the number of pedestrians stopped waiting in both systems for the High-High (a) and High-Low (b) scenarios.

Figures 10a and 10b illustrate vehicle waiting times under both scenarios. Figure 10a shows that the intelligent system reaches a peak of waiting vehicles between 8 and 15 minutes due to higher pedestrian traffic affecting vehicle flow. In contrast, Figure 10b indicates a peak at around 15 minutes when pedestrian traffic is lower, allowing the system to balance vehicle and pedestrian phases better.

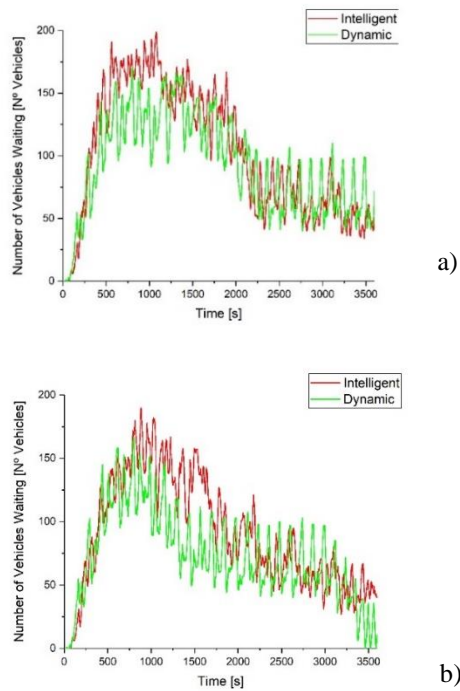


Figure 10. Comparison of the number of cars in the entire environment for both systems for the High-High (a) and High-Low (b) scenarios.

Despite both scenarios having high vehicle traffic, the intelligent system manages fewer waiting vehicles in the low pedestrian scenario. The dynamic system shows consistent behavior with a 120-second cycle time, but the high pedestrian count negatively impacts vehicle dispatch, suggesting that many waiting pedestrians might lead to poor vehicle flow.

VII. CONCLUSIONS

This paper sets the groundwork for advancing intelligent traffic management by highlighting the potential of VLC technology to enhance safety and efficiency at urban intersections. Our focus was on optimizing both vehicular and pedestrian traffic, addressing the previously overlooked aspect of pedestrian phases. By analyzing agents' behavior and decision-making, particularly concerning pedestrian safety, we aimed to refine the timing of pedestrian phases.

In the domain of traffic optimization, our state representation incorporates environmental information, vehicle and pedestrian distribution data from V-VLC messages, and a proposed phasing diagram guiding agent actions. We developed dynamic and intelligent control system models to securely manage traffic at two connected intersections. Through Reinforcement Learning and the SUMO simulator, we conducted a thorough analysis. With an agent at each intersection, the system optimizes traffic lights based on communication from VLC-ready vehicles, devising strategies to enhance flow and coordinate with other agents for overall traffic optimization.

Overall, the intelligent system demonstrates superior adaptability and efficiency. It manages to reduce pedestrian waiting times while still maintaining a reasonable level of vehicle flow. In comparison, the dynamic system's fixed cycle often leads to longer pedestrian wait times, which can cause significant congestion. Therefore, the intelligent system proves to be more effective in handling the traffic scenarios studied, providing a better balance between vehicle and pedestrian needs.

ACKNOWLEDGMENT

This work was sponsored by FCT – Fundação para a Ciência e a Tecnologia, within the Research Unit CTS – Center of Technology and Systems, reference UIDB/00066/2020 and by IPL project reference IPL/IDI&CA2024/NUTRAMISEL.

REFERENCES

- [1] D. O'Brien et al., "Indoor Visible Light Communications: challenges and prospects," Proc. SPIE 7091, 709106, pp. 60-68, 2008.
- [2] X. Liang, X. Du, G. Wang, and Z. Han, "A Deep Reinforcement Learning Network for Traffic Light Cycle Control," in IEEE Transactions on Vehicular Technology, vol. 68, no. 2, pp. 1243-1253, Feb. 2019, doi: 10.1109/TVT.2018.2890726.
- [3] I. Sousa, P. Queluz, A. Rodrigues, and P. Vieira, "Realistic mobility modeling of pedestrian traffic in wireless networks". In 2011 IEEE EUROCON-International Conference on Computer as a Tool, pp. 1-4, IEEE, 2011.
- [4] T. Ding, S. Wang, J. Xi, L. Zheng, and Q. Wang, "Psychology-Based Research on Unsafe Behavior by Pedestrians When Crossing the Street". Adv. Mech. Eng., 7, 203867, pp. 1-6, 2015.
- [5] J. Oskarbski, L. Guminska, M. Miszewski, and I. Oskarbska., "Analysis of Signalized Intersections" in the Context of Pedestrian Traffic. Transportation Research Procedia, 14, pp. 2138-2147, 2016, doi:10.1016/j.trpro.2016.05.229
- [6] Y. Elbaum, A. Novoselsky, and E. A. Kagan, "Queueing Model for Traffic Flow Control in the Road Intersection," Mathematics, 10, 3997, 2022. doi: 10.3390/math10213997.
- [7] S. Yousefi, E. Altman, R. El-Azouzi, and M. Fathy, "Analytical Model for Connectivity in Vehicular Ad Hoc Networks," IEEE Transactions on Vehicular Technology, 57, pp. 3341-3356, 2008.
- [8] Alvarez Lopez et al., "Microscopic Traffic Simulation using SUMO. In: 2019 IEEE Intelligent Transportation Systems Conference (ITSC), pp. 2575-2582. IEEE. The 21st IEEE International Conference on Intelligent Transportation Systems, Maui, USA, pp. 4.-7, Nov. 2018.
- [9] A. Yousefpour et al., "All one needs to know about fog computing and related edge computing paradigms: A complete survey", Journal of Systems Architecture, vol. 98, pp. 289-330, 2019.
- [10] M. A. Vieira, M. Vieira, P. Louro, and P. Vieira, "Cooperative vehicular visible light communication in smarter split intersections," Proc. SPIE 12139, Optical Sensing and Detection VII, 1213905, 17 May 2022; doi: 10.1117/12.2621069.
- [11] M. A. Vieira, G. Galvão, M. Vieira, M. Véstias, P. Vieira, and P. Louro, "Traffic Signaling and Cooperative Trajectories based on Visible Light Communication," Sensors and Electronic Instrumentation Advances, pp. 23, 2023.
- [12] M. A. Vieira, G. Galvão, M. Vieira, P. Louro, M. Vestias, and P. Vieira, "Enhancing Urban Intersection Efficiency: Visible Light Communication and Learning-Based Control for Traffic Signal Optimization and Vehicle Management". Symmetry 2024, 16, 240. https://doi.org/10.3390/sym16020240.
- [13] G. Galvão et al., "Traffic signals and cooperative trajectories at urban intersections: leveraging visible light communication for implementation," Proc. SPIE 12906, Light-Emitting Devices, Materials, and Applications XXVIII, 129060O (13 March 2024); doi : 10.1117/12.3000529.